In Situ Generated Turbostratic Graphite: A New Family of Self Lubricating Iron Based Composites

C. Binder[*], R Binder[**], D.R. Consoni[*], G. Hammes[*], R. Schroeder[**], A.N. Klein[*], J.D B. de Mello[*,***]

[*] Materials Laboratory (LabMat), Federal University of Santa Catarina, EMC, Florianópolis, SC, Brazil.
[**] Whirphool / Embraco, Joinville, SC, Brazil
[***] Laboratory of Tribology and Materials, Federal University of Uberlândia,Uberlândia, MG, Brazil,
d.mello@labmat.ufsc.br / ltm-demello@ufu.br

ABSTRACT

In this paper we present a new processing route able to produce a homogeneous dispersion of *in situ* generated, solid lubricant particles in the volume of sintered composites produced by metal injection molding. Thermal debinding and sintering were performed in a single thermal cycle using a Plasma Assisted Debinding and Sintering (PADS) process. Nodules of graphite (size ≤ 20μm) presenting a nanostructured stacking of graphite foils with thickness of a few nanometers were obtained. Micro Raman spectroscopy and TEM analysis indicated that the graphite nodules are composed of a so-called turbostratic 2D graphite which has highly misoriented graphene planes separated by large spaces. The effects of precursor content, metallic matrix composition and sintering temperature are presented and discussed. The results clearly show the great tailoring ability of the proposed micro-structural model. Moreover, the optimized processing parameters produced outstanding new iron based composites.

Keywords: turbostratic graphite, composites, *in situ*, self lubricating, tribological behaviour.

1 INTRODUCTION

In this work, we present a synthesis of the main results obtained from an ongoing research program that aims to develop new, low cost, iron based self lubricating composites, which combine low friction coefficient, high mechanical strength and wear resistance [1-6]. In this context, we have recently proposed [7] a new microstructural model taking into account the mean free path between solid lubricant particles and the active area covered by the lubricant particles. The high mechanical and tribological performances of the composites are a result of the combination of matrix mechanical properties and structural parameters. Special emphasis is given to a new processing route able to produce a homogeneous dispersion of *in situ* generated, discrete solid lubricant particles in the volume of sintered steels produced by metal injection molding.

2 EXPERIMENTAL TECHNIQUES

Iron based composites were produced by mixing carbonyl iron powder with elemental powder of the alloying elements. Different contents of silicon carbide powder (1, 2, 3, 4 and 5 wt% SiC) were added to the carbonyl iron powder. The thermal debinding, as well as the sintering, was performed in a single thermal cycle (Plasma Assisted Debinding and Sintering - PADS) [8-9].

In order to evaluate the influence of the matrix on the tribological behaviour, three different compositions of a 3% SiC composite (Fe-Si-C, Fe-Si-C-Ni and Fe-Si-C-Ni-Mo) were also produced. The processing routes are well described in previous works [2-3].

In all cases, the mechanical properties were evaluated by micro-hardness and tensile tests while the tribological behaviour was evaluated using two types of experiments:

a. Reciprocating sliding tests were conducted at constant normal load to access the friction coefficient and wear rates of specimens and counter-bodies.
b. Reciprocating sliding tests were carried out in an incremental loading mode. In this case, by increasing the normal load in increments of 7 N at 10 min. intervals, the scuffing resistance was determined. In this study, the scuffing resistance was defined as the work (N.m) at which the value of the friction coefficient first rose above 0.20 (lubricity effect).

In both kind of experiments, a hard steel AISI 52100 ball (diameter 10 mm) was fixed on a pivoted arm and rested against the specimen surface under constant stroke (5 mm) and frequency (2 Hz). The tests were conducted under controlled relative humidity (50 %) and temperature (22±4 °C).

Wear scars and microstructures were analyzed by using SEM-EDX, FEG-SEM as well as TEM; micro Raman spectroscopy and laser interferometry.

3 RESULTS AND DISCUSSION

Fig. 1 presents typical aspects of the microstructures.

The reference alloy presented a microstructure constituted of perlite (P) + ferrite (α), Fig. 1a, whereas the addition of SiC to the feedstock powder induces the formation of graphite nodules. The graphite nodules (G) are always surrounded by ferrite (α) rings, Fig. 1b. Such

microstructure formation was expected based on thermodynamic considerations and its evolution depends on sintering time and temperature, as well as on the amount of SiC. This is well described in a recent paper [6]. The remaining carbon forms graphite nodules (size ≤20 µm) which present a nanostructured stacking of graphite layers a few tenths of nanometres thick, Fig. 1c (obtained from a cryogenically fractured surface) and Fig. 1d.

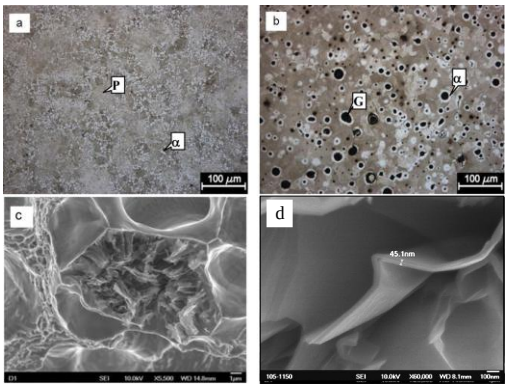

Figure 1: Typical aspects of the microstructure. Alloy Fe+0.6C+4 Ni. (a) Metallic matrix; (b) 2% SiC; (c) graphite nodule; (d) graphite layer.

The influence of the precursor content and of the sintering temperature on the steady state friction coefficient under a constant normal load is synthesized in Fig. 2.

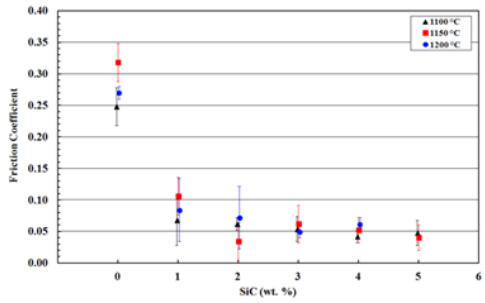

Figure 2: Effect of the silicon carbide content and sintering temperature on the friction coefficient. *The x values were slightly shifted (±0.02) to the left and right.*

Independently of the sintering temperature, an increase of the precursor content, which increased the number of graphite nodules, reduced the average friction coefficient. In general, the reduction was substantial (up to 3% SiC). For higher SiC contents, the friction coefficient was almost constant. It is also noticeable that the friction coefficient was hardly affected by the sintering temperature. All composites showed a considerably smaller friction coefficient than the matrix alloys (graphite-free alloys).

In a previous paper [2], we concluded that there was, definitely, no correlation associating the friction coefficient with the mechanical properties of the composites. Instead, we explained the outstanding tribological behaviour of these newly developed sintered composites based on the presence of the so-called turbostratic 2D graphite, which accordingly to the literature, has longer interlamellae distances than the highly oriented 3D graphite. We supposed that graphite foils were removed from the *in situ* generated graphite nodules and remained at the interface, which formed a protective tribolayer. Because of the small size of the powders in MIM processes, the mean free path among the graphite nodules was also small, and the "coverage" of the surface among the nodules was easily achieved.

To further understand this point, a few other types of graphite were analysed under the same tribological configuration: They are graphite nodules in a nodular cast iron, and the contact was submerged in graphite in powder. The matrix alloy (graphite-free - Fe 0.6 % C) was also tested as a reference.

Fig. 3 shows the average friction coefficient (steady state) of different materials.

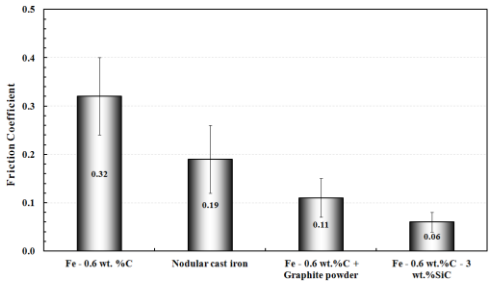

Figure 3: Effect of graphite type on friction coefficient. The matrix alloy (graphite-free - Fe 0.6 % C) was added as a reference.

The reference alloy presented the highest friction coefficient. The presence of graphite (nodules in nodular cast iron and graphite in powder) strongly reduced the friction coefficient. The addition of 3 % SiC further reduced the friction coefficient and induced a remarkably low value (0.04).

Figure 4 presents the typical Raman spectra of different graphite types. They clearly show a G band at approximately 1580 cm^{-1}. Graphite associated with graphite powders and nodular cast iron is characterised as 3D graphite and is highly aligned according to the literature [7]. The spectrum of the graphite nodules produced by the SiC decomposition (Fig. 4-a) clearly presents a widened G band (associated with the sp^2 hybridisation) and a D band (associated with crystallinity disorder).

The analysis of the spectra [2,7] clearly shows many evidence (the widening of the bands, the ID/IG ratio, the size of the graphite crystallites and the shape of the second-order G' band) of the presence of the so called turbostratic 2D graphite which has highly misoriented graphene planes separated by large spaces.

The large inter planar distance (≥ 3.499 Å against 3,354 Å for the high aligned 3D graphite) among the graphene foils and misorientation of the graphene foils has been confirmed by transmission electron microscopy, as

illustrated in figure 5, and is, probably, the origin of the low friction coefficient.

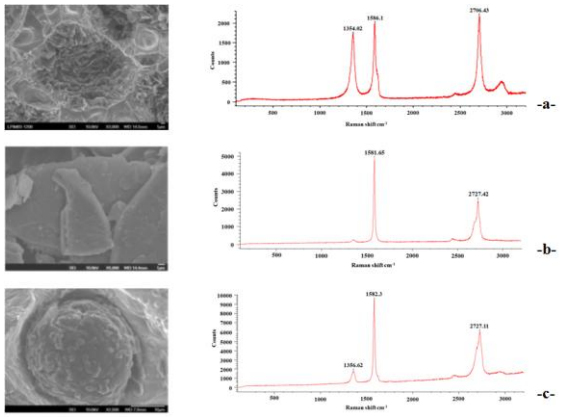

Figure 4: Typical Raman spectrum. (a) Graphite nodule obtained via the SiC decomposition. (b) graphite in powder. (c) Graphite nodule in nodular cast iron.

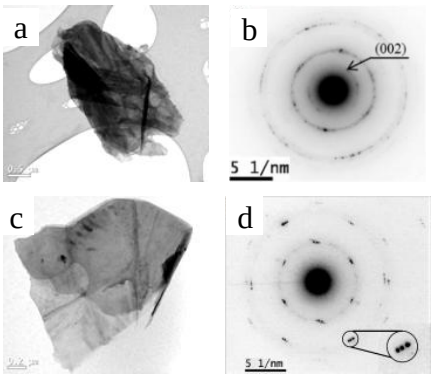

Figure 5: Typical TEM results. (a) and (c) bright fields of turbostratic graphite layers. (b) SAED showing the interlamellae space. (d) SAED showing the graphene foils misorientation.

These large spaces among the graphene planes drastically decrease the interaction among the planes, which results in a low shear strength. Thus, it is reasonable to suppose that during the reciprocating sliding, the graphite planes shear easily and maintain a constantly lubricated contact interface.

On the contrary, the sintering temperature strongly influences scuffing resistance, Fig. 6. The low sintering temperature induces significantly higher scuffing resistance (5x). In order to further understand why the low sintering temperature induced higher scuffing resistance, the samples sintered at 1100 ◦C were cryogenically fractured and then the surfaces were analyzed using SEM [2]. The analysis showed the presence of partially dissolved SiC particles within the graphite nodules. Taking into account that the metallic matrix is continuous it is reasonable to suppose that the solid lubricant, or its precursor, does not contribute to the mechanical resistance of the composite. However, the presence of undissociated particles of SiC may produce a greater load bearing capacity and the protection of the matrix/tribolayer, thus inducing higher scuffing resistance.

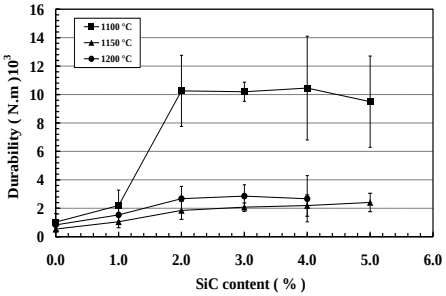

Figure 6: Effect of SiC content and of sintering temperature on the scuffing resistance.

The addition of alloying elements to the composites produced different matrices. All three microstructures have in common the presence of graphite nodules, induced by the addition of SiC to the feedstock powder, whereas the metallic matrix varies from ferrite to martensite. The reference alloy (Fe + 0.6% C) presented a matrix constituted mostly of ferrite (stabilized by Si), with a very small fraction of perlite. Addition of Nickel did not substantially change the microstructural constituents. For the Ni + Mo containing alloy, the metallurgical constituents changed from ferrite/perlite to martensite.

The influence of metallic matrix on the steady state friction coefficient is synthesized in Fig. 7.

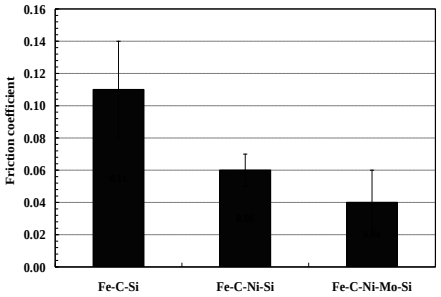

Figure 7: Effect of metallic matix on friction coefficient.

The addition of alloying elements considerably reduced the friction coefficient (45% reduction for the Ni alloys) and values as low as 0.04 were obtained (65% reduction) for the Fe-C-Ni-Mo steels.

Wear scars associated with the specimens presented different widths and the general appearance of the wear marks also varied. Inside the wear scar there was a clear evidence of abrasive wear, as evidenced by the presence of multiple parallel scratches [3]. The intensity and number of scratches varied according to the material. The wear loss of the counter-bodies presented the same behaviour as the specimens. The wear rate of specimens and counter-bodies is summarized in Fig. 8.

The lowest wear rates were found for the samples containing alloying elements. These reductions in the friction coefficient and in the wear of the tribological pair

may be associated with the tribofilm transfer effects from the self lubricating steel to the ball and vice-versa, and thus continuously avoiding the metal-metal contact and was linked to the resistance of the metallic matrix to plastic deformation and consequently, to the sealing of lubricant reservoirs [3].

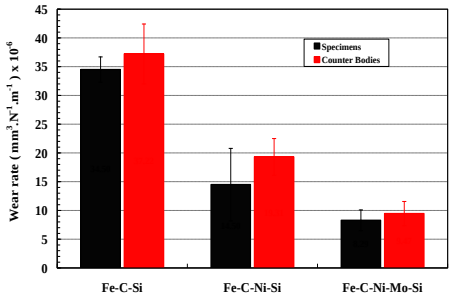

Figure 8: Wear rate of the self lubricating composites and AISI 52100 steel ball.

Fig 9.a and fig 9.b present the dominant spectra found in the wear scar of the Fe-C-Ni-Mo alloy. All spectra clearly show the presence of the so called turbostratic 2D graphite. It is also noticeable that the spectra of tribo layers presented in the wear scars of the specimens or in the counter-bodies are almost identical and indicate the beneficial presence of the turbostratic 2D graphite on both sides of the tribo pair.

On the contrary, the spectra found in the wear track of the reference alloy changed according to their position in the wear scar. Spectra similar to those found in the previous case were measured near the border of the wear scars, whereas those found in the centre of the scar were a little different, fig. 9.c and fig. 9.d. Despite presenting lower intensities of the 2D graphite characteristic bands and a certain amount of fluorescence, the spectra also presented other smaller bands at lower frequencies. The origin of these bands was attributed to the formation of iron oxide by tribochemical reaction caused by the surrounding atmosphere and is, probably, a consequence of the high energy availability associated with high friction coefficients. It is reasonable to suppose that the presence of iron oxides associated with the smaller intensities of the graphitic phase is likely to induce inferior tribological performance.

CONCLUDING REMARKS

In synthesis, the results clearly show the great tailoring ability of the proposed micro-structural model when applied to the development of self lubricating composites. Moreover, the optimized processing parameters produced outstanding new iron based composites,

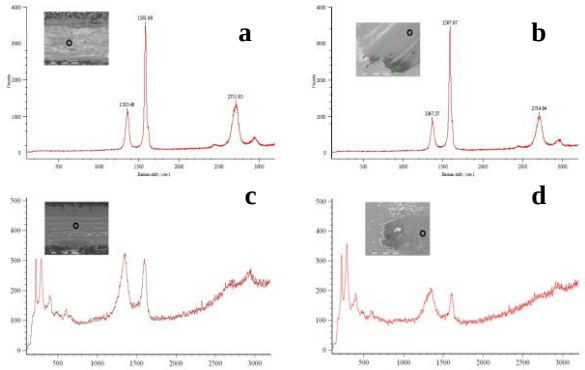

Figure 9: Typical Raman spectra. (a) Fe-C-Ni-Mo specimen. (b) Fe-C-Ni-Mo counter-body. (c) Fe-C specimen, centre of the scar. (d) Fe-C counter-body, centre of the scar.

REFERENCES

[1] Binder, C., Hammes, G., Schroeder, R., Klein, A. N., de Mello, J. D. B., Binder, R., Ristow, W., Metal Powder Report., 65, 29-37, 2010.

[2] De Mello, J.D.B., Binder, C., Binder, R., Klein, A. N., Wear, 271, 1862-1867,2011.

[3] De Mello, J. D. B., Binder, C., Hammes, G., Klein, A. N., Wear, 301, 648-655, 2013.

[4] Hammes, G., Schroeder, R., Binder, C., Klein, A. N., de Mello, J. D. B., Tribology International., 70, 119-127, 2014.

[5] R. Binder, C. Binder, W Ristow Jr, A. N. Klein, *Composition of particulate materials for forming self-lubricating products in sintered steels, product in self- lubricating sintered steel and process for obtaining self-lubricating products in sintered steel*, PI0805606-Brazil; US 20110286873A1-USA; International Number: WO 2010/069020 A2-Europe; CN102497948A-China; JP 2012-512320-Japan; 10-2011-0110179-South Korea; SG 172168 A1-Singapore, TW 201034773 A1-Taiwan.

[6] A.N. Klein, C. Binder, G. Hammes, J.D.B. de Mello, W. Ristow, R. Binder, , in: Proceedings of EURO PM2009, Vol. 1, 191–196, 2009.

[7] K. R Campos, P. Kapsa, C. Binder A.N. Klein, J.D.B. de Mello, *"Tribological evaluation of self-lubricating sintered steels"*, Wear, *in press*, 2015.

[8] A.N. Klein, J.L.R.A. Muzart, R. Souza, M.C. Fredel, P.A.P. Wendhausen, R.M. Nascimento, , US patent (US 6,579,493 B1), 2003.

[9] R. Machado, J.L.R. Muzart, A.N. Klein, W. Ristow, M.C. Fredel, P.A.P. Wendhausen, D. Fusao, L. Mendes, PCT (WO 2006012718) and INPI (PI-0403536-4), 2004.